RESILIENT INFRASTRUCTURE
June 1–4, 2016
RESILIENT INFRASTRUCTURE LONDON 2016

BOND STRENGTH OF RIBBED-SURFACE HIGH-MODULUS GLASS FRP BARS EMBEDDED INTO UNCONFINED UHPFRC

Mahmoud Sayed-Ahmed
Ryerson University, ON

Khaled Sennah
Ryerson University, ON

ABSTRACT

High-modulus (HM) ribbed-surface glass fiber reinforced polymer (GFRP) bars have recently been used in concrete bridge decks to avoid corrosion of steel reinforcement resulting from the use of de-icing salts in winter times in North America. Recently, prefabricated full-depth deck panels (FDDPs), made of normal strength concrete or high performance concrete and reinforced with GFRP bars, are used in Canada to acceleration bridge construction. The FDDPs are connected through panel-to-panel and panel-to-girder connections. These connections are filled with joint-filled cementitious materials as ultra-high performance fiber-reinforced concrete (UHPFRC). This paper presents the experimental program to investigate the bond strength of the GFRP bars embedded into unconfined UHPFRC using pull-out testing, leading to the proper GFRP bar development length required to determine the width of the closure strip between connected slabs. The longitudinal GFRP/UHPFRC interface is influenced by (i) the development length-to-nominal diameter of the bar ratio, (ii) the concrete cover-to-bar diameter ratio and (iii) the development length-to-embedment depth ratio due to lugs or headed-end and (iv) concrete compressive strength. GFRP bars embedded into UHPFRC would rely less on the friction and adhesion of the interface, and more on the bearing of the lugs against the concrete. These bearing forces act at an angle to the axis of the bar, causing radial outward forces. Pullout failure of the GFRP/UHPFRC interface leads to shearing of the lugs and bar slippage from the headed-end. Adequate bond strength between the GFRP/UHPFRC interfaces is necessary for design of jointed PDDFs. Therefore, accurate predictions of development length and bond strength of straight or headed-end bars without passing through the high localized stresses due to flexural are essential for safe design.

Keywords: Ultra-High Performance Fibre Reinforced Concrete (UHPFRC), Glass FRP (GFRP), Pullout, development length, Design Codes, Experimental Testing, Accelerated Bridge Construction.

1. INTRODUCTION

To accelerate bridge construction while maintaining high level of long-term durability and reduction in the maintenance cost, design engineers recently considered utilizing UHPFRC, which possesses high compressive and tensile strength compared to normal strength concrete. Also, they recently considered the use of GFRP bars for the same rationale. GFRP-UHPFRC structural section works together through (i) bonding between GFRP bars and surrounding UHPFRC that prevents slip of the bar relative to UHPFRC, (ii) concrete mix design that provides the structural member with high concrete capacity design loads, and (iii) similar rates of thermal expansion for the UHPFRC to the GFRP bars under environmental conditions.

UHPFRC is made by mixing ordinary Portland cement, supplementary cementitious materials as the Silica Fume, fine aggregate as ground quartz, steel fiber reinforcement, admixtures as the high range water reducer (HRWR), and water (Graybeal, 2006 and 2007). UHPFRC is a self-consolidated concrete with high fluidity and deformation capability that levels itself without vibration. Its strength increases with age and curing, with early compressive strength of 100 MPa at 96 hours (4 days), 140 MPa at 28 days, and 150 MPa by the 56 days. The curing regime for the untreated concrete is meant to keep the concrete into the capped-plastic moulds in the lab-room condition.

GFRP bar has high tensile strength-to-weight ratio compared to the steel reinforcement, in addition to its corrosion resistance that increases structure's service life. GFRP is anisotropic material that provides high strength in the direction of the fibers, and low shear strength perpendicular to the axes of the bar. The bar exhibits linear elastic load until failure with no yielding point as that for steel reinforcement, thus design should account for the lack of ductility. The external surface of the GFRP bar may be ribbed-surface, sand-coated surface, wrapped with sand coated, deformed, or helical to achieve the desired bonding to the surrounding concrete. GFRP bars manufactured with straight end, headed anchor end, or 180˚ hook. GFRP is classified into low modulus (LM) and high modulus (HM) types based on the value of the bar modulus of elasticity.

The concept of the accelerated bridge construction and rapid bridge replacement introduces the prefabricated bridge elements and systems. Bridge elements are manufactured in plant, transported, installed on-site with casted-in-place joints by high early-strength concrete in order to open the traffic for traffic within few days. Recently, prefabricated full-depth deck panels (FDDPs), made of normal strength concrete or high performance concrete and reinforced with GFRP bars, are used in Canada to acceleration bridge construction. FDDPs are connected through panel-to-panel and panel-to-girder connections. These connections are filled with UHPFRC (Sayed-Ahmed and Sennah, 2014; Sayed-Ahmed et al., 2014). The bond strength of the development and spliced lengths of the HM-GFRP bars embedded into UHPFRC-filled closure strip between connected precast deck panels needs experimental investigations to determine the reasonable width for the panel-to-panel connection for cost-effective design.

Bond strength of GFRP bars is a mean to transfer the force in the reinforcement to the surrounding concrete. The interacting force at the bar-concrete interface may arise from (i) chemical adhesion and friction at the surface area of the bar connected to concrete, and (ii) bearing of the ribs or lugs that act at an angle to the axis of the bar, causing radial outward forces, counterpart with the surrounding concrete. Bond strength due to tensile loading fails under pullout of the bar, progressive splitting of concrete, or the combined failure modes. Flexural bond (i.e. *localized interaction*) generates high localized stress due to the rate of change of longitudinal tensile force along the span adjacent to the flexural cracks, and is proportional in magnitude to the change in flexural shear along the joint. Thus, the localized stress condition doesn't directly correlate to the development-length-related strength of the member. Equation [1] determines the horizontal force equilibrium that depends on the magnitude of $(T_D - T_{D'})/dz$). In this equation, u_s is the localized surface stress over nominal contact area between the steel bar and the concrete, d_b is the diameter of the single bar, u_b is the localized bearing stress over the area A_{br} per unit length between the lugs and the concrete (Wang and Salmon, 2002).

[1] $$u_s \pi d_b dz + u_b A_{br} dz = T_D - T_{D'}$$

ACI 318 (2015) defines the development length concept as the attainable average bond stress over the length of embedment of the reinforcement. The development length is a function of (i) the development length-to-nominal diameter of the bar ratio (l_d/d_b), (ii) the development length-to-concrete cover ratio (l_d/c_{min}), (iii) the development length-to-embedment depth ratio (l_d/h_{ef}) due to lugs, headed-end or the 180˚ hook, and (iv) the concrete compressive strength (f_c'), for confined and unconfined sections.

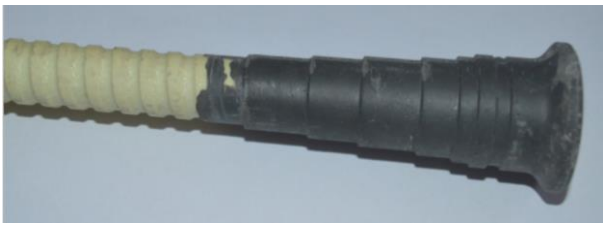

(a) Headed-end for ribbed-surface bar

(b) Ribbed-surface bar

Figure 1: Views of the ribbed-surface GFRP bar

This paper presents a summary of an experimental investigation on the direct tensile pullout load for the ribbed-surface GFRP bars, shown in Figure 1, considering different embedment lengths, namely: $4d_b$, $6d_b$, $8d_b$ and different concrete cover of 40, 90, and 140 mm under centric and eccentric loading, where d_b is the bar nominal diameter. Figure 2 depicts the possible failure modes of the GFRP bars embedded into unconfined UHPFRC. It is

expected that pullout failure of the GFRP bar would dominate under pullout as UHPFRC has high concrete capacity design leading to no concrete splitting failure.

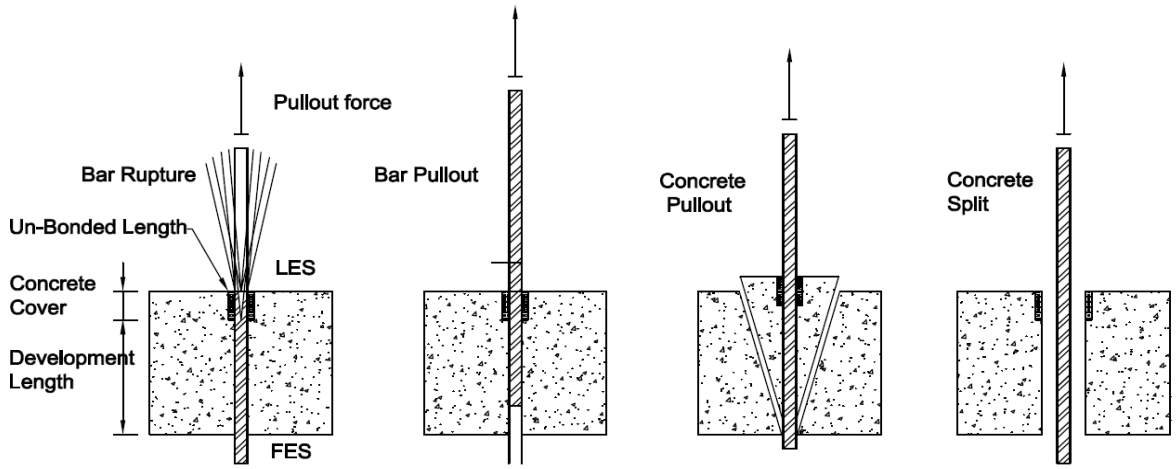

a.Bar rupture b. Bar pullout c. Concrete pullout d. Concrete split

Figure 2: Possible failure modes of GFRP bar embedded in concrete

2. EXPERIMENTAL WORKS

Tables 1 and 2 show the concrete constituent mix design, and the mechanical properties of UHPFRC, respectively, used in the current study. The OPC + SCM: Fine Aggregate: Water ratio is 1.33: 1.74: 0.20. Water-cement ratio can be reduced to reduce the fluidity of the mixture. Table 3 shows the material properties of the ribbed-surface GFRP bars used in this study. The length of the headed anchor for the ribbed-surface bar is 100 mm and its exterior diameter of the head anchor is 40 mm (Schoeck, 2011). Figures 3 and 4 show the bar locations either concentric or eccentric to the concrete block and the test setup, respectively. A 50 mm of unbonded lead length of the embedded bar shown in Figure 2 is meant to reduce the effect of the concrete breakout due to bar pullout and bearing due the placement of the test setup. Actual slip will eliminate the free end slip from the loaded end slip.

Table 1: Proportion of UHPFRC (Ductal) constituent materials **(Saleem , et al., 2013)**

Constituent materials	Percentage by weight (%)	Weight relative to cement
Portland cement	28.6	1.00
Silica fume	9.3	0.33
Ground quartz	8.5	0.30
Fine sand	41.1	1.44
Steel fiber reinforcement	6.4	0.22
Superplasticizer (HRWR)	0.5	0.02
Water	5.6	0.20
Total	100	

Note: Data from http://www.lafargnorthamerica.com (May, 2008).

Table 2: The UHPFRC (Ductal JS1000) physical properties

	Characteristic values for design		Design value
	Mean	Standard deviation	
	MPa	MPa	MPa
Compression	140	10	100
Flexural	30	5	
Direct tension	8	1	5
Young's modulus	50,000	2,000	45,000

Table 3: Material properties 15M and 20M straight bar (Schoeck, 2011)

	Tensile strength MPa	Strain %	Poisson's ratio	Effective cross-section with ribbed part, mm^2	Nominal cross-section, mm^2	Weight g/m	Nominal tensile modulus, GPa
15M	1188	2.61	0.20-0.22	254.47	201.06	0.53	64
20M	1188	2.61	0.20-0.22	380.13	314.16	0.53	64

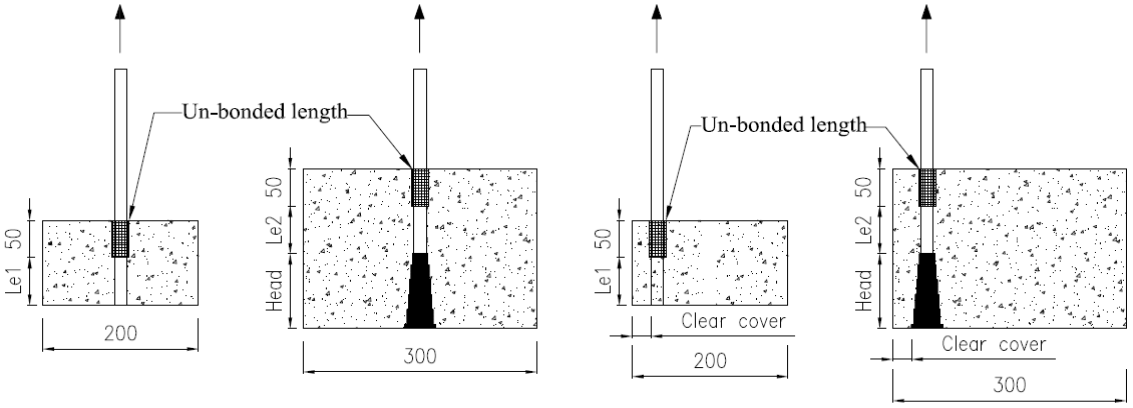

a) Straight bar b) Headed bar a) Straight bar b) Headed bar

Figure 3: Concentric and eccentric cube specimens

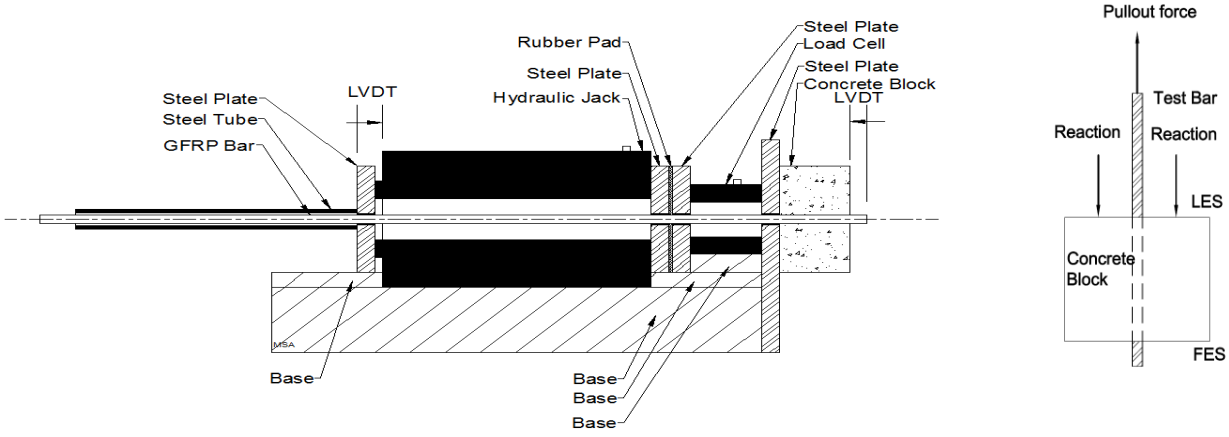

(a) Test Setup (b) Data location

Figure 4: Pullout test setup

1. PULLOUT TEST RESULTS

The specimens ID in Tables 4 to 6 represents (i) the bar location to the concrete block (C = Concentric, E = Eccentric), (ii) bar diameter (16 mm or 20 mm), (iii) embedment length ($4d_b$, $6\ d_b$, $8\ d_b$), (iv) bar type (S = Straight, H = Headed end) and (v) specimen number in a group. The static pullout loading was applied in a gradual increment by steel wedge friction grips. Data recorded the applied load, load-end slip (LES), and free-end slip (FES). The pullout failure mode was found to be due to (i) inter-laminar shear strength (ILSS) failure between the GFRP bar and its surface, along with slippage from the headed-end and (ii) shear-off failure of ribbed-surface. The relationship between pullout load and the embedment length-to-nominal diameter of the bar ratio (l_e/d_b) was found to be quadratic polynomial of the second degree, with parabola opens upwards. The vertex of the parabola, also called the turning point of such curve, is located at the mid points of the l_e/d_b series equal to 4, 6, 8, respectively. The normalized concrete compressive strength should be considered to account for its variation as $\sqrt{f_c'}$.

Table 4: Pullout test results for 15M ribbed-surface GFRP bar with centric & eccentric bar location

ID	d_b Mm	l_e Mm	Cover mm	f_c' MPa	P_{ult} kN	LES mm	FES Mm	Failure mode
C16.4d.S1	16	64	92	191.60	95.00	13.18	0.23	Pullout
C16.4d.S2	16	64	92		98.00	14.01	0.24	Pullout
C16.4d.S3	16	64	92		104.00	13.02	0.25	Pullout
C16.4d.S4	16	64	92		88.00	18.00	0.21	Pullout
C16.4d.S5	16	64	92		86.00	11.93	0.21	Pullout
Mean					**94.2**	**14.028**	**0.228**	
C16.6d.S1	16	96	92	191.86	62.00	16.22	0.26	Pullout
C16.6d.S2	16	96	92		61.00	16.46	0.28	Pullout
C16.6d.S3	16	96	92		53.00	14.42	0.25	Pullout
C16.6d.S4	16	96	92		54.00	22.14	0.16	Pullout
C16.6d.S5	16	96	92		69.00	17.99	0.21	Pullout
Mean					**59.8**	**17.446**	**0.232**	
C16.8d.S1	16	128	92	191.86	84.00	25.81	0.53	Pullout
C16.8d.S2	16	128	92		77.00	28.58	0.23	Pullout
C16.8d.S3	16	128	92		73.00	30.52	0.40	Pullout
C16.8d.S4	16	128	92		76.00	23.49	0.41	Pullout
C16.8d.S5	16	128	92		63.00	19.47	0.21	Pullout
Mean					**74.6**	**25.574**	**0.356**	
C16.0d.H1	16	100	142	168.53	115.00	18.00	0.28	Pullout
C16.0d.H2	16	100	142		125.00	14.00	0.30	Pullout
C16.0d.H3	16	100	142		123.00	14.00	1.30	Pullout
C16.0d.H4	16	100	142		133.00	12.00	1.41	Pullout
C16.0d.H5	16	100	142		115.00	16.00	0.28	Pullout
Mean					**122.2**	**14.8**	**0.714**	
E40-16.4d.S1	16	64	40	191.86	93.00	12.68	0.37	Pullout
E40-16.4d.S2	16	64	40		101.00	13.67	0.35	Pullout
E40-16.4d.S3	16	64	40		95.00	22.05	1.01	Pullout
E40-16.4d.S4	16	64	40		93.00	16.27	0.18	Pullout
E40-16.4d.S5	16	64	40		103.00	15.33	0.17	Pullout
Mean					**97**	**16**	**0.416**	
E40-16.6d.S1	16	96	40	191.60	74.00	24.94	0.38	Pullout
E40-16.6d.S2	16	96	40		88.00	28.74	0.45	Pullout
E40-16.6d.S3	16	96	40		75.00	25.17	0.38	Pullout
E40-16.6d.S4	16	96	40		68.00	22.21	0.35	Pullout
E40-16.6d.S5	16	96	40		58.00	16.10	0.24	Pullout
Mean					**72.6**	**23.432**	**0.36**	
E40-16.8d.S1	16	128	40	191.86	109.00	26.43	0.66	Pullout
E40-16.8d.S2	16	128	40		89.00	26.19	0.72	Pullout
E40-16.8d.S3	16	128	40		73.00	22.29	0.33	Pullout
E40-16.8d.S4	16	128	40		75.00	23.24	0.24	Pullout
E40-16.8d.S5	16	128	40		80.00	19.28	0.48	Pullout
Mean					**85.2**	**23.486**	**0.486**	
E40-16.0d.H1	16	100	40	170.77	131.00	18.00	0.51	Pullout
E40-16.0d.H2	16	100	40		132.00	18.14	0.51	Pullout
E40-16.0d.H3	16	100	40		114.00	16.00	0.44	Pullout
E40-16.0d.H4	16	100	40		119.00	17.00	0.48	Pullout
E40-16.0d.H5	16	100	40		114.00	16.00	0.46	Pullout
Mean					**122**	**17.028**	**0.48**	

The 15M straight bar with centrically-loaded specimens and with l_e/d_b series equal to 4, 6 and 8 exhibits average ultimate load, P_{ult}, of 94.2, 59.8 and 74.6 kN, respectively, as shown in Table 4. The corresponding average critical load-end slip was found to be 14.028, 17.446 and 25.574 mm while the critical values for the free-end slip was found to be 0.228, 0.232 and 0.356 mm for the same series arrangement, respectively. The 15M headed-end bar

recorded pullout load, LES and FES as 122.2 kN, 14.8 mm and 0.714 mm, respectively. The bar manufacturer reported that bars with headed ends yield a mean value of the tensile strength / embedment strength between 100 and 110 kN, and the characteristic value of the tensile strength is above 80 kN, with tensile stress above 400 MPa (Schoeck, 2011).

The 15M straight bar with 40 mm eccentrically-loaded specimens and l_e/d_b series equal to 4, 6 and 8 exhibits average ultimate load, P_{ult}, of 97, 72.6 and 85.2 kN, respectively, as shown in Table 4. The corresponding average critical load-end slip values were found to be 16, 23.432 and 23.486 mm while the critical values for the free-end slip were found to be 0.416, 0.36 and 0.486 mm for the same series arrangement, respectively. The 15M headed-end bar recorded pullout load, LES, FES as of 122 kN, 17.028 mm and 0.48 mm, respectively. The 15M straight bar with 60 mm eccentrically-loaded specimens and l_e/d_b series equal to 4, 6 and 8 exhibits average ultimate load, P_{ult}, of 51.8, 64.4 and 81.2 kN, respectively, as shown in Table 5. The corresponding average critical load-end slip values were found to be 17.928, 16.542 and 26.428 mm while the critical values for the free-end slip were found to be 0.238, 0.282 and 0.856 mm for the same series arrangement, respectively.

The 20M straight bar with centrically-loaded specimens and l_e/d_b series equal to 4, 6 and 8 exhibits average ultimate load, P_{ult}, of 59.4, 115.4 and 127 kN, respectively, as shown in Table 6. The corresponding average critical load-end slip values were found to be 15.492, 18.966 and 27.614 mm while the critical values for the free-end slip were found to be 0.29, 0.784 and 0.274 mm for the same series arrangement, respectively. Unlike the polynomial behaviour of the 15M, the 20M follows downward parabola with turning point at l_e/d_bequals to 6 with hair cracks into the concrete blocks. The 20M straight bar with 40 mm eccentrically-loaded specimens and with l_e/d_b series equal to 8 exhibits average critical load, LES and FES as 117.4 kN, 23.278 mm and 0.296 mm, respectively, with observed hair cracks into the concrete blocks.

In summary, the straight and/or headed-end GFRP embedded into unconfined UHPFRC fails due to shear-off failure of the ribbed-surface (lugs) for the straight bar, and bar slippage from the headed anchor as shown in Figure 5. Experimental data is provided to build up needed databases for future and further detailed analysis.

Table 5: Pullout test results for ribbed-surface 15M with 60 mm eccentric bar location

ID	d_b	l_e	Cover	f_c'	P_{ult}	LES	FES	Failure mode
	Mm	mm	mm	MPa	kN	mm	mm	
E60-16.4d.S1	16	64	60		45.00	18.38	0.26	Pullout
E60-16.4d.S2	16	64	60		49.00	19.60	0.19	Pullout
E60-16.4d.S3	16	64	60	191.60	55.00	16.16	0.24	Pullout
E60-16.4d.S4	16	64	60		46.00	16.53	0.22	Pullout
E60-16.4d.S5	16	64	60		64.00	18.97	0.28	Pullout
Mean					**51.8**	**17.928**	**0.238**	
E60-16.6d.S1	16	96	60		83.00	19.60	0.37	Pullout
E60-16.6d.S2	16	96	60		53.00	19.00	0.24	Pullout
E60-16.6d.S3	16	96	60	191.60	60.00	19.00	0.27	Pullout
E60-16.6d.S4	16	96	60		55.00	16.00	0.25	Pullout
E60-16.6d.S5	16	96	60		71.00	9.11	0.28	Pullout
Mean					**64.4**	**16.542**	**0.282**	
E60-16.8d.S1	16	128	60		83.00	26.24	0.33	Pullout
E60-16.8d.S2	16	128	60		78.00	28.88	0.55	Pullout
E60-16.8d.S3	16	128	60	192.39	86.00	25.25	0.38	Pullout
E60-16.8d.S4	16	128	60		84.00	24.88	0.37	Pullout
E60-16.8d.S5	16	128	60		75.00	26.89	2.65	Pullout
Mean					**81.2**	**26.428**	**0.856**	

Table 6: Pullout test results for ribbed-surface 20M with centric and eccentric bar location

ID	d_b	l_e	Cover	f_c'	P_{ult}	LES	FES	Failure mode
	Mm	mm	mm	MPa	kN	mm	mm	
C20.4d.S1	20	80	90		66.00	17.86	0.31	Pullout
C20.4d.S2	20	80	90		58.00	15.69	0.27	Pullout
C20.4d.S3	20	80	90	191.86	45.00	12.18	0.21	Pullout
C20.4d.S4	20	80	90		63.00	16.91	0.29	Pullout
C20.4d.S5	20	80	90		65.00	14.82	0.37	Pullout
Mean					**59.4**	**15.492**	**0.29**	
C20.6d.S1	20	120	90		128.00	20.21	0.50	Pullout
C20.6d.S2	20	120	90		133.00	21.44	0.52	Pullout
C20.6d.S3	20	120	90	191.06	123.00	19.83	0.48	Pullout
C20.6d.S4	20	120	90		97.00	15.64	2.04	Pullout
C20.6d.S5	20	120	90		96.00	17.71	0.38	Pullout
Mean					**115.4**	**18.966**	**0.784**	
C20.8d.S1	20	160	90		133.00	26.38	0.25	Pullout
C20.8d.S2	20	160	90		133.00	26.38	0.25	Pullout
C20.8d.S3	20	160	90	191.60	147.00	29.15	0.27	Pullout
C20.8d.S4	20	160	90		109.00	33.85	0.39	Pullout
C20.8d.S5	20	160	90		113.00	22.31	0.21	Pullout
Mean					**127.00**	**27.614**	**0.274**	
E40-20.8d.S1	20	160	40		119.00	20.35	0.61	Pullout
E40-20.8d.S2	20	160	40		117.00	27.22	0.33	Pullout
E40-20.8d.S3	20	160	40	191.86	112.00	22.91	0.22	Pullout
E40-20.8d.S4	20	160	40		108.00	22.38	0.12	Pullout
E40-20.8d.S5	20	160	40		131.00	23.53	0.20	Pullout
Mean					**117.4**	**23.278**	**0.296**	

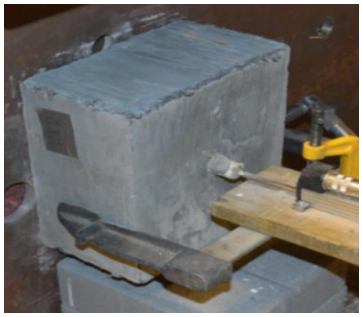

(a.1) UHPFRC Block

(a.2) Shearing of ribs

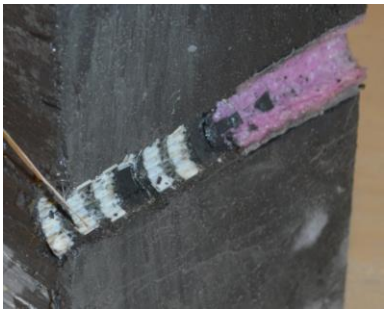

(a.3) Section cut

(a) Ribbed-surface bars

(b.1) Bar slippage

(b.2) Bar slippage from the headed anchor

(b) Headed-end bars

Figure 5: Typical observed failures of GFRP embedded into UHPFRC

3. ANALYTICAL STUDY

The ACI318 basic approximate method is used to determine the embedment length through Equations [1] to [3]. Equation [2] is used to determine the experimental / empirical coefficient, k. ACI318 assumed that the factor $k_d > k_{experimental}$, where this coefficient ensures that it will be larger than all measured embedment lengths and yields to conservative development length, l_d. Due to the fact that the actual strength of GFRP is greater than the nominal value, the development length was based on multiplication of the modification factor (MF) to the nominal fracture strength ($MF = 1.0\ to\ 1.30$); that considers bar location with respect the concrete cover.

[1] $$u\,\pi\,d_b\,l_e = A_b\ f_{frp,ultimate}$$

[2] $$l_e = k_{exp}\,(A_b\ f_{frp,ultimate})/\sqrt{f_c'}$$

[3] $$k_{exp} = \sqrt{f_c'}/(u\,\pi\,d_b)$$

[4] $$l_d = MF \times k_d\,(A_b\ f_{frp,ultimate})/\sqrt{f_c'}$$

The development length for hooked or headed-end bars in tension should be obtained by multiplying the basic hook/headed development length, l_{hb}, shown in Equations 5 and 6, by appropriate modification factors (MF); that is

[5] $$l_{hb} = MF \times 100\ \frac{d_b}{\sqrt{f_c'}}$$

However, l_{hb}, should not be less than $8d_b$ or 150 mm, whichever is greater.

[6] $$k_{hb} = \frac{l_{dh}\sqrt{f_c'}}{A_b\,f_{frp,u}}$$

Table 7: ACI318 basic factor, k_{exp} for ribbed-surface HM GFRP bars

Loading location	Bar type	Bar diameter	l_e/d_b	ACI basic factor, k_{exp}
Centric	Straight	16	4.00	0.00371
	Straight	16	6.00	0.00557
	Straight	16	8.00	0.00742
	Headed-end	16	6.26	0.00543
Eccentric at 40 mm	Straight	16	4.00	0.00371
	Straight	16	6.00	0.00556
	Straight	16	8.00	0.00742
	Headed-end	16	6.25	0.00547
Eccentric at 60 mm	Straight	16	4.00	0.00371
	Straight	16	6.00	0.00556
	Straight	16	8.00	0.00743
Centric	Straight	20	4.00	0.00297
	Straight	20	6.00	0.0044
	Straight	20	8.00	0.00593
Eccentric at 40 mm	Straight	20	8.00	0.00594

The ACI basic development factor for the straight-ended ribbed-surface HM GFRP bar, k_d, equals to 0.00743 and 0.00594 for the 15M and 20M bars, respectively, as shown in Table 7. These k_d factors for the same bar arrangement are equivalent to 33.995% and 31.456% of the bar maximum ultimate strength of 1188 MPa, yielding actual tensile stresses of 403.86 and 373.69 MPa for the 15M and 20M bars, respectively. Thus, the development length would be 150 mm and 190 mm for the 15M and 20M bars, respectively, if embedded into UHPFRC with

nominal compressive strength of 140 MPa as shown in Equations 7 to 9. The calculations for the l_d resulted into minimum l_d of 9.5 times bar diameter for the 15M and 20M straight bars. Larger diameter straight bars require longer embedment length.

[7] $l_d = MF \times k_d \, (A_b \; f_{frp,ultimate})/\sqrt{f_c'}$

[8] $l_d = 1.0 \times 0.00743 \, (201 \times 1188 \,)/\sqrt{140}$ = 150 mm

[9] $l_d = 1.0 \times 0.00594 \, (314 \times 1188 \,)/\sqrt{140}$ = 190 mm

Table 8: Bond factors and development length of HM GFRP bars embedded into UHPFRC

Type	Size	Diameter, mm	k	$f_c' = 140MPa$	
				l_d, mm	l_{hb}, mm
Straight	15M	16	0.00743	150	--
Straight	20M	20	0.00594	190	--
Headed	15M	16	82	--	111

The ACI basic development factor for the headed-end HM GFRP bar is k_{hb}equals to 0.00547 for the 15M bar. The k_{hb} factor is equivalent to 51.076% of the bar maximum ultimate tensile strength of 1188 MPa, yielding actual tensile stress of 606.78 MPa before the bar slips from the anchor. Thus, the basic development for the 15M headed-end bar embedded into concrete with compressive strength of 140 MPa results into l_{hb} would equal to 111 mm per Equations 10 and 11. The calculations for the l_{hb} resulted into minimum development length of 7 times the bar diameter.

[10] $l_{hb} = 0.00547 \, \frac{A_b f_{frp,u}}{\sqrt{f_c'}} = 0.00547 \, \frac{\pi \, d_b}{4} f_{frp,u} \frac{d_b}{\sqrt{f_c'}} = 82 \, \frac{d_b}{\sqrt{f_c'}}$, where d_b = 16 mm

[11] $l_{hb} = 82 \, \frac{d_b}{\sqrt{f_c'}}$

4. CONCLUSIONS

Based on the experimental observations and analysis of the test results, the following conclusions can be drawn:

1. The allowable bar slip at loaded-end and free-end of the GFRP bars should be limited with acceptable range as bar fails suddenly due to shear-off failure of the bar surface or bar slippage from the anchor head.
2. For straight GFRP bars, the minimum development length of 9.5 times the bar diameter or 152 mm whichever is greater is recommended.
3. For headed-end GFRP bars, the minimum development length of 7 times the bar diameter or 112 mm whichever is greater is recommended.
4. A Modification Factor for bar location in UHPFRC can range from 1 to 1.3 representing bar location with large concrete cover (representing centric location in the concrete block) to 40 mm concrete cover (representing eccentric location of the block).

ACKNOWLEDGMENTS

This study was sponsored by Ontario Ministry of Transportation's Highway Infrastructure Innovation Funding Program (MTO-HIIFP) through cash contribution, Lafarge North America for supplying raw materials of the UHPFRC, Schoeck Canada Inc. for supplying GFRP bars. Opinions expressed in this paper are those of the authors and do not necessarily reflect the views and policies of the Ministry or the participating companies.

REFERENCES

ACI318-15. 2015. *Building code requirements for reinforced concrete,* Detroit, MI: American Concrete Institute.

Graybeal, B. A. 2006. *Material Property Characterization of Ultra-High Performance Concrete, Publication No. FHWA-HRT-06-103.,* Mclean, VA.: U.S. Department of Transportation. Federal Highway Administration.

Graybeal, B. A. 2007. Compressive Behaviour of Ultra-High-Performance-Fibre-Reinforced Concrete. *ACI Materials Journal ,* 104(2): 146-152.

Saleem , M. A., Mirmiran, A., Xia, J., and Mackie, K. 2013. Development Length of High-Strength Steel Rebar in Ultra-High Performance Concrete. *Journal of Materials in Civil Engineering, 25:* 991-998.

Sayed-Ahmed, M. and Sennah, K. 2014. *Development of transverse joints for full-depth precast deck panels incorporating ribbed-surface GFRP bars and UHPFRC.* Proceedings of the 2014 PCI Convention and National Bridge Conference, National Harbour, MD, pp 1-10.

Sayed-Ahmed, M., Sennah, K., and Lai, D., 2014. *Development of transverse joints for full-depth precast normal-strength concrete deck panels incorporating ribbed-surface GFRP bars and UHPFRC.* Proceedings of the 9th International Conference on Short and Medium Span Bridges, Calgary, Alberta, pp 1-10.

Schoeck Canada Inc. 2011. *ComBar Technical Information.* [Online] Available at: www.Schoeck-Canada.com.

Wang, C. K., and Salmon, C. G. 2002. *Reinforced Concrete Design, Sixth Edition.* USA: John Wiley & Sons, Inc.